Electrochimica Acta 92 (2013) 276–284

Contents lists available at SciVerse ScienceDirect

Electrochimica Acta

journal homepage: www.elsevier.com/locate/electacta

The effect of dopant pK_a and the solubility of corresponding acid on the electropolymerisation of pyrrole

Eimear M. Ryan[a,b], Carmel B. Breslin[a], Simon E. Moulton[b,*], Gordon G. Wallace[b]

[a] Department of Chemistry, National University of Ireland Maynooth, Co. Kildare, Ireland
[b] ARC Centre of Excellence for Electromaterials Science, Intelligent Polymer Research Institute, University of Wollongong, NSW 2522, Australia

ARTICLE INFO

Article history:
Received 30 January 2012
Received in revised form
26 November 2012
Accepted 26 November 2012
Available online 5 December 2012

Keywords:
Electropolymerisation
Polypyrrole
pH effects
Diclofenac sodium salt
Valproic acid sodium salt

ABSTRACT

In this paper, attempts to dope polypyrrole (PPy) with two small sized anionic drugs, diclofenac sodium salt (NaDF) and valproic acid sodium salt (NaVPA), are described. For PPy doped with DF^-, unusual patterns in growth and morphology were observed. During the deposition of the polymer, the rate of electropolymerisation decreased with increasing time and higher applied potentials. The polymer had features of an insulating film, while SEM confirmed the presence of crystal-like shards on the surface of the polymer. Analyses of these crystals indicate them to be drug that may have precipitated out of solution. These findings suggest that insoluble drug crystals are formed during electropolymerisation. The formation of PPy doped with a small soluble anti-epilepsy anionic drug, VPA^-, was also studied; however it was not possible to incorporate this drug during electrochemical polymerisation. Again, this was explained in terms of the equilibrium between the anion and the acid forms of VPA. At pH values below 5.6, the equilibrium of the VPA^- is shifted towards the insoluble HVPA. As the monomer is oxidised, there is a decrease in the local pH in the vicinity of the electrode and this causes the HVPA to precipitate from solution. This, in turn, prevents any PPy from being deposited at the electrode.

1. Introduction

PPy is by far the most extensively investigated conducting polymer (CP) not only due to the fact that the pyrrole (Py) monomer is easily oxidised, water soluble and commercially available but also because of its environmental stability, good redox properties and the ability to give high electrical conductivities [1]. PPy can be prepared both chemically and electrochemically.

The electrochemical oxidation of Py can be achieved using different electrical stimuli including constant current, constant potential and cyclic voltammetry (CV). Otero and De Larreta [2] noted that the choice of electrochemical method has an influence on the morphology, appearance and adhesion of the PPy film. The films formed from a constant current or constant potential mode of electropolymerisation are generally more porous and uneven than those achieved by CV, which are smooth and compact. However, more recent studies have shown that PPy films formed potentiostatically have a smooth surface morphology and the growth of the polymer is easier to control [3].

The anions present in the supporting electrolyte are incorporated during the electropolymerisation process [4] and these can affect the morphology, porosity and redox properties of the deposited PPy [5]. Dopants of various sizes have been studied including Cl^-, ClO_4^-, NO_3^-, para-toluene sulfonate (pTS^-) and dodecyl benzene sulfonate (DBS^-) [4,6–9]. When deposited PPy is doped with smaller anions, such as Cl^-, ClO_4^- and NO_3^-, anion exchange is mainly displayed, in the course of the film charging and discharging in the background electrolyte solution, due to the high mobility of these ions in the polymer matrix. Cation exchange generally takes place on PPy modified with large and bulky anions, such as DBS^-. However, when counterions are medium in size, like pTS^-, PPy exhibits both anion and cation exchange behaviour. In addition, pronounced effects of a large ion size were observed for tetraphenylborate in deposition of PPy [4] and polyanions (tungstosilicic) for PANI [10]. The electrolyte concentration is also important with Li and Yang [11] reporting that the doping, conductivity and tensile strength of a NO_3^- doped PPy film increase as the electrolyte concentration increases until a concentration of 1.0 M is reached. Beyond that no improvement was observed.

The temperature also plays an important role in the electropolymerisation of Py. A decrease in redox properties of PPy is observed as the temperature during polymerisation increases [12]. Although the rate of the electropolymerisation reaction is increased with increasing temperatures, the PPy that is deposited on the electrode is more likely to become over-oxidised and this has an insulating effect which hinders the further growth of the PPy.

Although the monomer oxidation potential is independent of the pH, the pH has an effect on the reactivity and stability of

* Corresponding author. Tel.: +61 2 4298 1443; fax: +61 2 4221 3114.
E-mail address: smoulton@uow.edu.au (S.E. Moulton).

0013-4686/$ – see front matter © 2012 Elsevier Ltd. All rights reserved.
http://dx.doi.org/10.1016/j.electacta.2012.11.115

the PPy formed at the electrode [13]. In general, protons are produced after each oxidation at the electrode which consequently decreases the pH near the electrode. Zhou and Heinze [14] investigated the influence of pH on electropolymerisation of Py from acetonitrile and found that neutral or weakly acidic pH favours polymerisation. This is consistent with Pletcher and co-workers [15] who also found this to be the case when preparing a PPy film at a Pt electrode from solutions of varying pH. In addition, pH affects the speed of electropolymerisation with PPy forming rapidly in acidic conditions, slower in neutral pH, and not forming at all in basic solutions. A very low pH results in the formation of a film of low conductivity. This is due to the acid catalysed formation of non-conjugated trimers which further react to form a partly conjugated PPy or become incorporated into the film [16]. At basic conditions, cation radicals become deprotonated to neutral radicals which interfere with the radical–radical coupling reaction [17]. During synthesis the pK_a of all species is important as the pH selected will influence which ions are present. It may be necessary to select a pH, which is a compromise between the rate of electropolymerisation and the nature of the dopant species in the electrolyte solution.

PPy has been identified as a promising material for biomedical devices not only due to its light weight and ability to function at body temperature, but also its ability to exhibit a reversible electrochemical response. It can also work as an ion-gate which, in turn, allows the polymer film to bind and expel ions in response to electrical signals [18]. This makes PPy ideal for applications in controlled drug delivery. Diclofenac sodium salt (NaDF) belongs to the non-steroidal anti-inflammatory class of drugs (NSAID) and is one of the most effective of these in the treatment of musculoskeletal pain, such as arthritis and acute injury [19]. Sodium valproate (NaVPA) is the sodium salt of valproic acid and is an anticonvulsant used in the treatment of epilepsy as well as other psychiatric conditions requiring the administration of a mood stabiliser.

From the literature, it is clear that the development of a device that could ensure the correct dose of NaDF and NaVPA to be delivered to a desired area of the body is imperative. For example, implanting a NaDF containing device directly into the knee joint of an arthritis sufferer, would not only result in quick and effective pain relief, but would also circumvent the gastrointestinal side effects that many long term users suffer from. The ability to implant a NaVPA loaded device into the brain of an epilepsy sufferer would permit the precise delivery of therapeutic levels of the anticonvulsant to control the onset of seizures. In addition this target delivery approach would overcome the many side effects associated with current systemic anticonvulsant delivery routes. Reports have documented that such drug delivery systems are being studied whereby NaDF and NaVPA can be encased in chitosan hydrogels [20,21], albumin microspheres [22], agar beads [23] or degradable polycaprolactone [24]. However, in these systems the drug is not released in response to a trigger mechanism but at a steady rate over a given time. While time-dependent drug release may be suitable for some patients, it is not an ideal method to administer drugs and can lead to further issues with toxicity. To the best of the author's knowledge, there are no reports in the literature of the incorporation of VPA^- and DF^- into polypyrrole by electrochemical means.

In this paper, diclofenac sodium salt, (NaDF) and valproic acid sodium salt (NaVPA) are chosen as model dopant systems, as the pK_a values of the corresponding weak acids, HDF and HVPA, are 4.15 and 4.8, respectively. The influence of these dopants on the rate of electropolymerisation is examined, while the morphology of the deposited film is analysed in terms of the equilibrium between the anionic and the acid forms of the dopants.

2. Experimental

Diclofenac sodium salt (NaDF), valproic acid sodium salt (NaVPA) and paratoluene sulfonic acid sodium salt (pTS) were purchased from Sigma–Aldrich and used without any further purification. The Py monomer (98%) was purchased from Aldrich and distilled prior to use and stored at −4 °C.

All potentiostatic, galvanostatic and CV experiments were carried out using either a Solartron (Model SI 1285) or an EDAQ potentiostat, in a standard three electrode cell, with a high surface area platinum wire as the auxiliary electrode and a saturated calomel electrode (SCE), Ag/AgCl or silver wire as the reference electrodes. The SCE and Ag/AgCl electrodes were used in all experiments carried out at room temperature, while at 50 °C a silver wire was used as the reference. A platinum (Pt) disc electrode (99.99% purity) with a surface area of 0.125 cm^2 and gold coated Mylar (surface area = 1 cm^2), were used as the working electrodes. Gold Mylar is a flexible polyester sheet that has been coated in a thin layer of gold and was purchased from CPFilms Inc. (USA). The Pt disc electrode was made by embedding a Pt rod in epoxy resin in a Teflon holder and electrical contact was achieved by a wire threaded into the base of the metal sample. The exposed surfaces were polished to a mirror finish, using successively smaller sizes of diamond paste, down to a final size of 1 μm, rinsed with distilled water and finally cleaned in an ultrasonic bath to remove any residues from polishing. The gold Mylar was washed in ethanol and pre-treated in a UV-ozone cleaner (UV PRO 2800) for 20 min to remove any contaminants on the surface.

The polypyrrole films were prepared from a 0.20 M Py solution containing different concentrations of the dopants with no other electrolyte and at potentials ranging between 0.70 and 0.90 V vs. SCE. In addition, cyclic voltammetry and galvanostatic experiments were employed in an attempt to deposit the VPA-doped polypyrrole. Scanning electron microscopy (SEM) was performed on a JEOL JSM7500FA cold Field Emission Gun Scanning Electron Microscope (FEGSEM). Energy Dispersive X-ray (EDX) analysis of PPyDF film was performed to ascertain the elemental composition of the film using a Bruker EDS system (XFlash® 4010 Silicon Drift Detector from Bruker AXS Inc.) with Esprit 1.9 software. Fourier Transformed Infrared–Attenuated Total Internal Reflection (FTIR–ATR) Spectroscopic (Shimadzu prestige 21) utilising a germanium (Ge) ATR crystal was used to characterise the synthesised PPyVPA polymer films.

All EQCM experiments were carried out on a CHi440 EQCM and the equipment consisted of a quartz crystal oscillator, a frequency counter, a fast digital function generator, a high resolution and high speed data acquisition circuitry, a potentiostat and a computer. The polymers were deposited onto polished Au quartz crystal electrodes (Cambria Scientific) with an exposed surface area of 0.203 cm^2. The electrochemical cell consisted of a specially made Teflon holder in which the crystal was placed between two o-rings. During each experiment only one of the metal electrode surfaces is in contact with the electrolyte. The quartz crystal is supported by two wires, one to carry current to the gold layer and the other to allow for crystal vibration and to record the frequency. The set up is completed using a platinum wire counter and a custom-made Ag|AgCl reference electrode.

3. Results and discussion

3.1. Solubility and ionised state of the dopants

It is reported by the manufacturer that the solubility of NaDF in water is 50 g L^{-1} at room temperature and it has a pK_a of 4.15. The experimental conditions were chosen to ensure that this anion

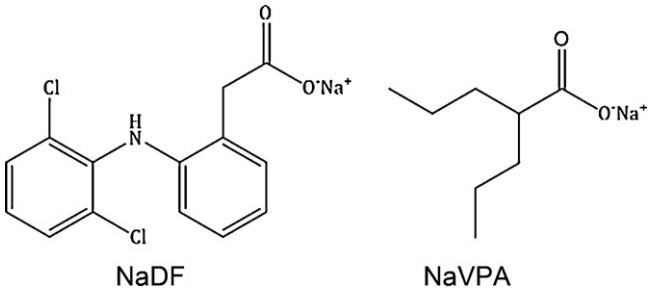

Fig. 1. Chemical structures of diclofenac sodium salt (NaDF) and valproic acid sodium salt (NaVPA).

was incorporated into the PPy and therefore a high concentration of the DF was used. Furthermore, the anionic, DF^-, species is more soluble in water than the HDF species. The well-known Henderson Hasselbalch equation was used to compute the % of anions in solution. NaDF, shown in Fig. 1, will be fully ionised in water, Eq. (1). However, in the presence of H^+ the anionic DF^- is partially protonated and equilibrium between the neutral acid form, HDF, and the anionic DF^- exists, as shown in Eq. (2). The dissociation of the neutral HDF molecule to the anionic form, DF^-, is described in Eq. (2) and using this together with Eqs. (3) and (4), the % of anionic DF^- can be found as a function of pH.

$$DF^-Na^+ \rightarrow DF^- + Na^+ \quad (1)$$

$$DF^- + H^+ \rightarrow HDF \quad (2)$$

$$K = \frac{[DF^-][H^+]}{[HDF]} \quad (3)$$

$$\%[DF^-] = \frac{100}{1 + 10^{pK_a - pH}} \quad (4)$$

NaVPA, shown in Fig. 1, can be treated in a similar manner and the dissociation of NaVPA (pK_a of 4.8) can be described too in accordance with Eqs. (1)–(3). The influence of pH on the % of anions in solution for both dopants is highlighted in Fig. 2. It can be seen that HDF and HVPA are predominantly neutral at low pH values but become more anionic in nature as the pH of the solution is increased. The pH of the NaDF-containing Py solution and the NaVPA-containing Py solution was experimentally measured to be 7.4. At this pH, the % of DF^- and VPA^- anions in solution is 96% and 93% respectively (using Eq. (4) and the listed pK_a values) and the equilibrium favours the anionic form of DF and VPA.

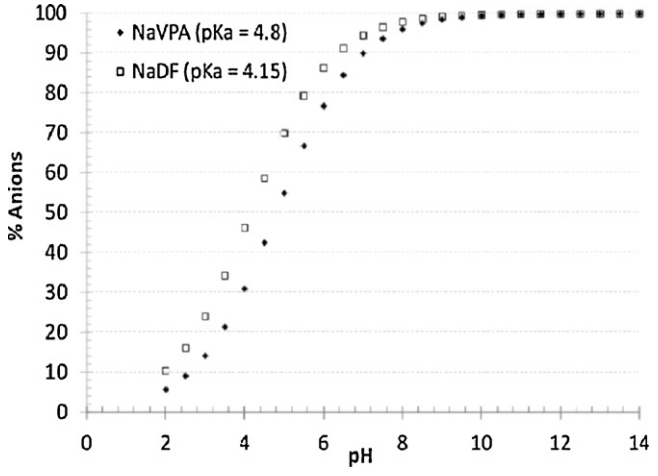

Fig. 2. The percentage of anions as a function of pH of NaDF and NaVPA. The % of anions for the given pH was calculated by substituting various pH values into Eq. (4).

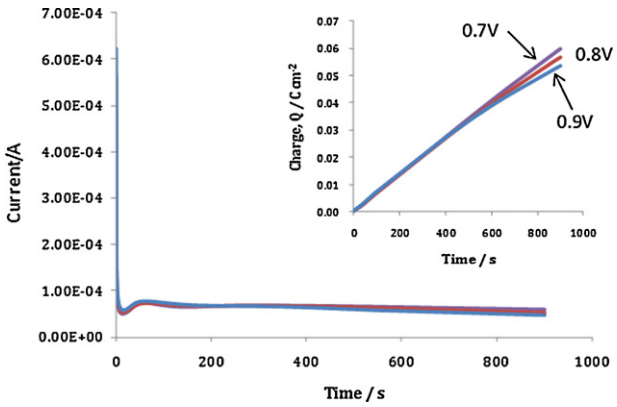

Fig. 3. Current–time plots recorded at Pt in the presence of 0.05 M NaDF and 0.20 M Py, at 0.70 V, 0.80 V and 0.90 V vs. SCE. Inset: Corresponding charge–time plots. Experiments were carried out at room temperature (RT).

3.2. PPy doped with DF^-

The electropolymerisation of Py in the presence of NaDF was studied in a 0.05 M NaDF and 0.02 M Py solution using Pt as the working electrode. Constant potentials of 0.70 V, 0.80 and 0.90 V vs. SCE were applied in an attempt to deposit PPy doped with DF^- anions. Fig. 3 shows the resulting potentiostatic plots, with both the recorded current and charge plotted as a function of the electropolymerisation period. Upon application of the potential, there is an initial charging current, which arises from the charging of the double layer. After 10 s there is an increase in faradaic current but within 100 s it begins to decrease and continues to drop reaching approximately 4.6×10^{-5} A cm^{-2} at 900 s. The initial increase in current suggests oxidation of the monomer and deposition of the polymer with the decrease in current thereafter indicating continued polymer growth. The applied potential seems to have little influence on the rate of electropolymerisation. Indeed, the charge is slightly lower at the higher potential of 0.90 V vs. SCE. This is somewhat unusual as the applied potential is well known to influence the rate of electropolymerisation, increasing as the applied potential is increased, and this has been well documented in the literature [15,25,26].

The concentration of NaDF was increased to 0.10 M with the solution being heated to 50 °C in a water bath to assist in dissolution of NaDF. The conductivity of the electrolyte was measured and compared to that of 0.10 M NaCl to ensure it was a suitable electrolyte. A conductivity of 4.40 mS was measured for 0.10 M NaDF, while the conductivity of 0.10 M NaCl was found to be 8.76 mS. This indicates that the NaDF electrolyte is indeed appropriate for electrochemistry and sufficiently conducting.

The potentiostatic current–time and charge–time plots for the formation of PPyDF at the Pt electrode in 0.10 and 0.15 M NaDF are shown in Fig. 4. A constant potential of 0.90 V vs. Ag|Ag$^+$ was applied and the solution temperature was maintained at 50 °C. At both concentrations, similar currents are reached by 400 s, approximately 1.6×10^{-4} A cm^{-2}. From the charge–time plot, shown in the inset of Fig. 4, it appears that it is the lowest NaDF concentration that gives rise to the highest charge and the more efficient rate of electropolymerisation. Again, this is somewhat different to the majority of reports which show an increase in the rate of electropolymerisation with increasing concentrations of dopant [11,27]. However, the data in Fig. 4 may be related to the solubility of the drug. At the higher concentrations, the solubility limit of the drug at the polymer–solution interface is easier to exceed, leading to the precipitation of the drug at the polymer interface and a decrease in the rate of polymer growth. It is clear from a comparison of Figs. 3 and 4

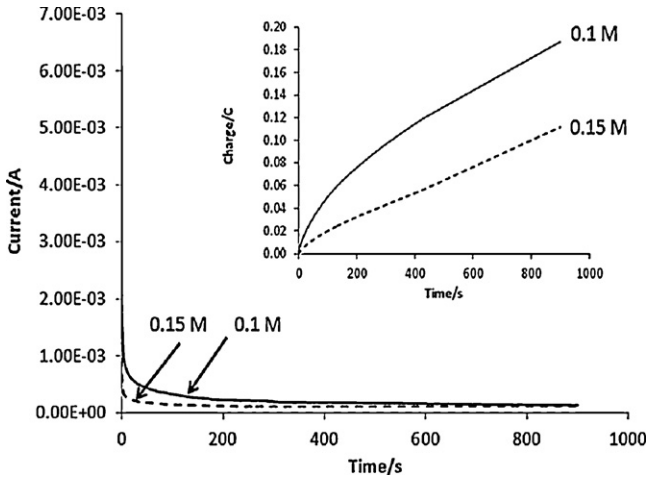

Fig. 4. Current–time plots recorded during the formation of PPyDF at 0.90 V vs. $Ag|Ag^+$ in 0.10 M, and 0.15 M NaDF in the presence of 0.20 M Py. Inset: Corresponding charge–time plots. Experiments were carried out at 50 °C.

that there is an increase in the rate of electropolymerisation at the higher temperature.

In view of the fact that a small amount of polymer was deposited on the bare electrode, a two-step method was developed. A film of PPy doped with pTS^- (PPypTS) was deposited to a charge of 0.70 C cm^{-2} and the PPy doped with DF^- was deposited by applying a constant potential for 20 min. Longer polymerisation times were not used as this could lead to the over-oxidation of the deposited polymer.

Current–time plots (Fig. 5A) and the corresponding charge–time plots (Fig. 5B) were recorded when the PPyDF film was deposited on a PPypTS film by applying potentials of 0.80 V vs. $Ag|Ag^+$ and 0.90 V vs. $Ag|Ag^+$ in the presence of 0.10 M NaDF and 0.20 M Py at 38 °C. The currents for the polymerisation at 0.80 V vs. $Ag|Ag^+$ are slightly higher. It is also clear from the charge–time plots that the polymer formed at 0.80 V vs. $Ag|Ag^+$ has a charge twice as high as that grown at 0.90 V vs. $Ag|Ag^+$. This indicates that more polymer is deposited at 0.80 V vs. $Ag|Ag^+$. The charge–time plots, shown in Fig. 5B, are not typical of the growth behaviour seen for PPy deposited from simple electrolytes [28–30]. For the initial growth of the polymer, the rate of electropolymerisation is constant, at 2.5×10^{-4} C cm^{-2} s^{-1}, but it then begins to deviate from this constant rate which suggests the rate of polymerisation decreases. This type of growth pattern is seen in insulating polymers [31,32] and suggests changes in the conductivity of the deposited polymer with continued electropolymerisation. It is also evident that the loss in conductivity is greater at the higher potential of 0.90 V vs. $Ag|Ag^+$.

3.3. Morphology of PPyDF

The morphology of PPy is well documented and in general it appears to have a cauliflower-like surface [33–35]. However, the micrograph of PPyDF, seen in Fig. 6, shows a distinctly different morphology. Crystal-like shards can be seen within the polymer matrix (Fig. 6A and B). Micrographs, taken at higher magnification, show that the polymer is deposited between the crystals. The cauliflower-like morphology of PPy is still evident between crystals, but the surface morphology is dominated by the crystals (Fig. 6C and D). These crystal-like shards and splints have not been reported in the literature in relation to the morphology of PPy. When EDX analysis was performed in a region where crystals are observed there is a large band associated with Cl indicating these crystals to be precipitated drug DF. EDX analysis of a polymer film (with no crystals present) showed the composition to be that of carbon,

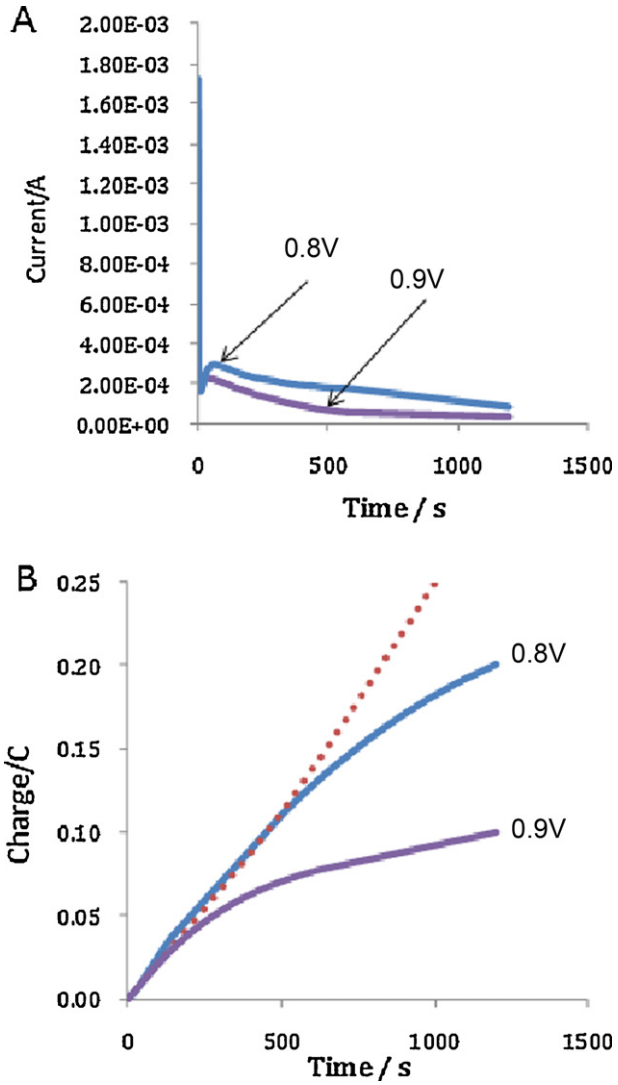

Fig. 5. Current–time plots (A) and charge–time plots (B) recorded in the presence of 0.10 M NaDF and 0.20 M Py at 0.80 V vs. $Ag|Ag^+$ and 0.90 V vs. $Ag|Ag^+$, deposited onto a thin film of PPypTS (deposited at Pt at 0.70 V vs. SCE to a charge of 0.70 C cm^{-2}). The charge–time growth profiles deviate from the initial rate of electropolymerisation (▪▪▪). Deposition of PPyDF was carried out at 38 °C.

nitrogen and chlorine with the presence of carbon and nitrogen being indicative of polypyrrole, while the presence of chlorine is due to DF retained in polypyrrole film (Fig. 6E). The inset of Fig. 6E shows the region of the PPyDF film that was analysed using EDX and show no crystal structures present, therefore the presence of the Cl band in the EDX must be coming from the DF that is doped into the PPy and not from any surface DF crystals.

As shown in Fig. 2, the % of DF^- anions calculated at the pH of the NaDF-containing Py solution, 7.4, is 96%. However, at lower pH values the equilibrium is shifted towards the insoluble HDF, as seen in Eq. (1). In the electropolymerisation of Py, Diaz et al. [36] proposed that the initial step is the generation of the radical cation. The coupling of two Py radicals results in the formation of a bond between the two α positions to give a radical dication. The loss of two protons generates a neutral dimer which is then oxidised to form a radical dimer. At this stage of polymerisation it is suggested that consecutive oligomerisation takes place via successive dimerization steps leading from a dimer to a tetramer and then to an octameric coupling product [37]. The increase in proton concentration during the electropolymerisation causes a local increase in the acidity at the interface of the electrode. Depending on the rate of

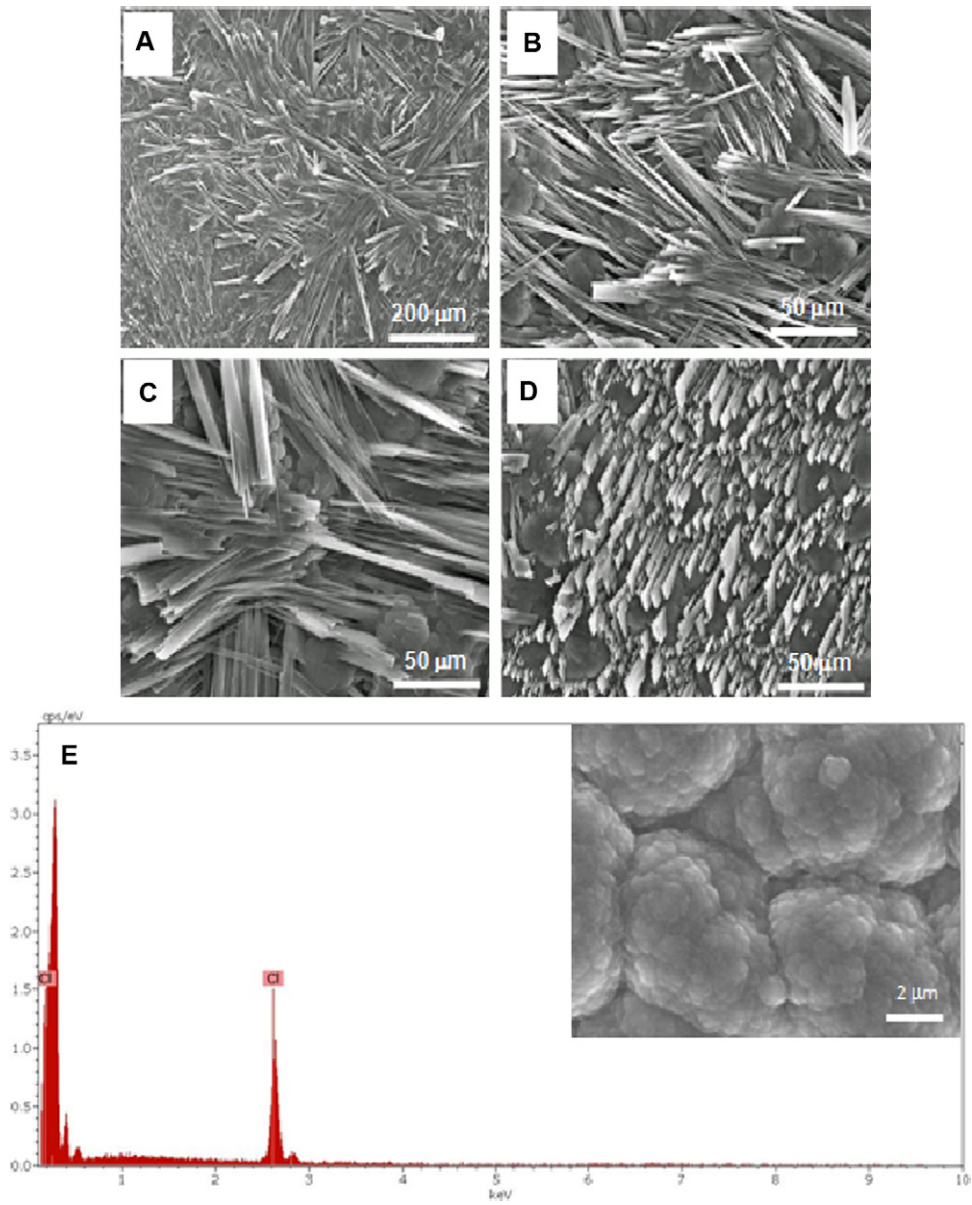

Fig. 6. SEM micrographs (A, B, C and D) of PPyDF electrodeposited onto a film of PPypTS. PPyDF was electrochemically polymerised in the presence of 0.10 M NaDF and 0.20 M Py at 38 °C. A potential of 0.80 V vs. $Ag|Ag^{+}$ was applied for 20 min. Energy Dispersive X-ray (EDX) analysis (E) of the PPyDF film (inset).

electropolymerisation, significant local pH changes can occur. For example, Rajeshwar and co-workers [38] used a micro-pH electrode to monitor the changes in pH during the formation of PPyCl and recorded pH values as low as 3.0 compared to the bulk pH of 5.6. This local acidification shifts the equilibrium of the DF^{-} anions in solution towards HDF. However, there is a sufficient concentration of DF^{-} anions in solution to facilitate polymer deposition, but the insoluble HDF drug crystals become entrapped within the polymer as it is deposited on the electrode surface. The rate of polymerisation is hindered by the presence of these crystals on the surface of the electrode as seen in the potentiostatic current–time plots and charge–time plots in Fig. 5.

3.4. Redox properties of the PPyDF

The redox properties of the PPyDF polymer deposited onto the PPypTS layer were probed using cyclic voltammetry (CV). A slow scan rate and low pH provide conditions under which CVs can be carried out [39–41]. The potential was swept between −1.20 V and 0.70 V vs. SCE at a scan rate of 25 mV s^{-1} in the presence of 0.10 M NaCl. Fig. 7A shows the resulting cyclic voltammograms recorded over 20 cycles. There is a broad reduction wave extending between −0.40 V and −1.00 V vs. SCE and there is also evidence of an oxidation peak at similar potentials on the forward cycle. The reduction peak below −0.8 V is unusual for PPy and may be the result of proton reduction due to the low pH of the electrolyte used. The polymer remains reasonably stable over the 20 cycles with little change in the voltammograms with continuous cycling. For comparative purposes, the PPyDF and PPypTS voltammograms are shown in Fig. 7B. The PPypTS was polymerised at 0.70 V vs. SCE and to a charge of 0.70 C cm^{-2}. The PPypTS CV shows oxidation and reduction peaks at approximately 0.07 V and −0.10 V vs. SCE, respectively. Another striking feature is the large capacitance exhibited by the PPypTS polymer compared to PPyDF. From this it is clear that the presence of the crystal-like structures in the PPyDF polymer has a significant effect on the electroactivity of the polymer, giving rise to a more insulating layer. Furthermore, it is clear that the deposition of the PPyDF onto the PPypTS film removes the electroactivity of

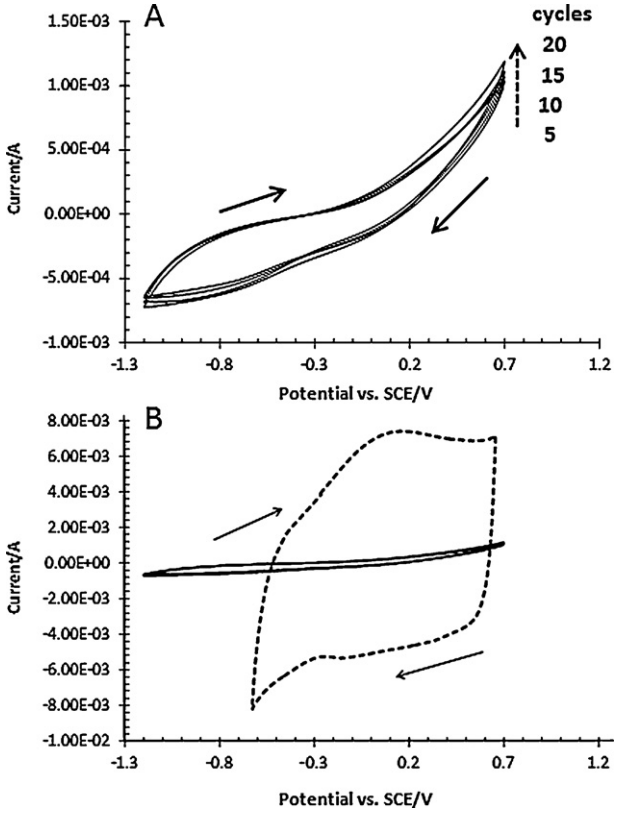

Fig. 7. Cyclic voltammograms recorded in 0.10 M NaCl for (A) PPyDF at 25 mV s^{-1} for 20 cycles with every 5th cycle shown and (B) PPypTS at 25 mV s^{-1}. The PPyDF was deposited on a film of PPypTS at 0.8 V vs. SCE from a solution of 0.10 M NaDF and 0.20 M Py at 38 °C. The PPypTS was deposited at 0.70 V vs SCE to a charge of 0.70 C cm^{-2} at RT.

the PPypTS. There is no evidence of the redox properties of the underlying PPypTS film in Fig. 7A.

3.5. Characterisation of PPy doped with DF by electrochemical quartz crystal microbalance (EQCM)

In EQCM measurements, the frequency of the oscillating quartz crystal is monitored. Changes in the frequency are observed as the mass of the crystal changes. The changes in frequency are related to the changes in mass through the Sauerbrey equation, Eq. (5) [42].

$$\Delta f = -\frac{2{f_0}^2 \Delta M}{A\sqrt{\rho\mu}} \quad (5)$$

Here, f_0 is the resonant frequency, ΔM is the mass change, A is the surface area of the electrode, 0.203 cm^2, ρ is the density of the quartz, 2.648 g cm^{-3}, and μ is the shear modulus of the quartz, 2.947×10^{11} g cm^{-1} s^{-2}. In this equation the change of frequency (Δf) is equal to minus the change in mass (ΔM) per unit area (A) times a constant. The frequency, therefore, decreases as the mass increases. EQCM was employed to study the initial deposition process of the PPyDF. Using the Sauerbrey equation, Eq. (5), the shift in the resonant frequency of the crystal was then used to calculate the mass of the polymer. This equation assumes the current efficiency for the electropolymerisation of pyrrole is 100% and that no water is incorporated into the film [43]. The PPyDF polymer was deposited directly onto the Au on the quartz crystal as the presence of the underlying polymer film (prelayer) resulted in the film being too thick and subsequently deviations from the Sauerbrey equation, Eq. (5), were observed. Accordingly, in these studies, the

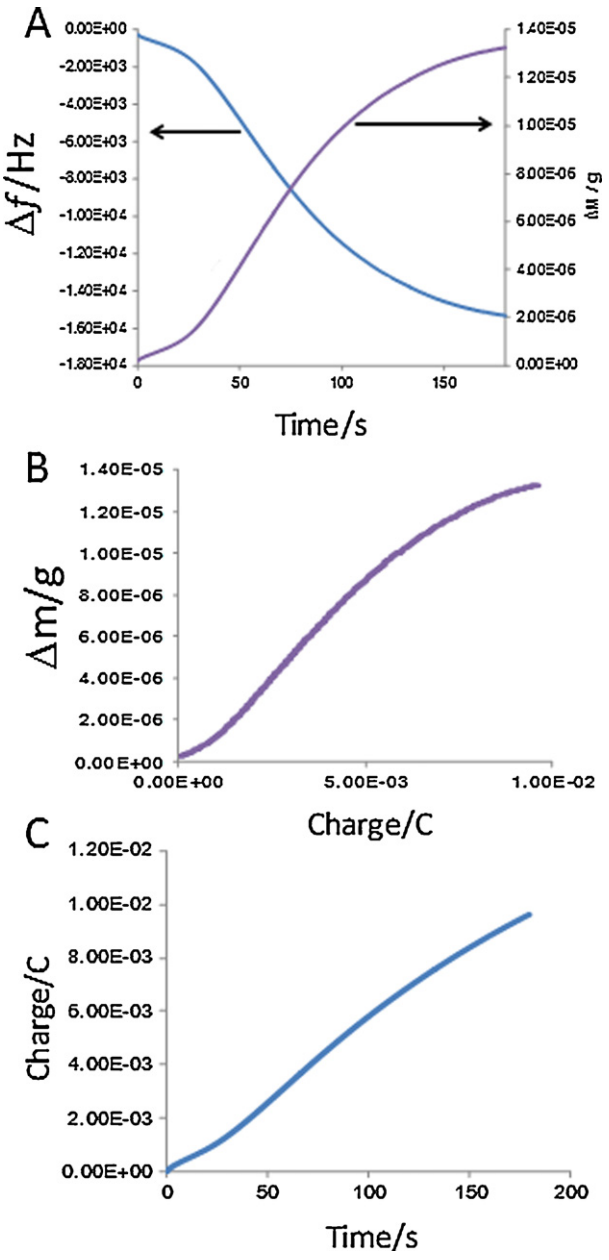

Fig. 8. Frequency and mass (A) recorded during the formation of PPyDF in the presence of 0.10 M NaDF and 0.20 M Py at a potential of 0.80 V vs. Ag|AgCl until a charge of 9.6×10^{-3} C was consumed. (Area = 0.208 cm^2). Mass–charge plot (B) and charge–time plot (C) recorded during the deposition of the PPyDF film on Au quartz crystal electrode in the presence of 0.10 M NaDF and 0.20 M Py. (Area of quartz crystal = 0.208 cm^2).

PPyDF was deposited directly onto the Au quartz crystal electrode until a charge of 1.20×10^{-2} C was consumed.

The changes in frequency of the crystal and the corresponding mass changes as the PPyDF film is deposited are shown in Fig. 8A. This growth profile can be divided into three segments, an initial period of about 30 s, where very small quantities of polymer are deposited. This corresponds to the initial nucleation of the polymer at the gold surface. This is then followed by a period where the polymer is deposited at a much higher rate. Finally, after approximately 150 s, the rate of deposition decreases again. Representative mass–charge and charge–time plots are shown in Fig. 8B and C respectively and show a very clear nucleation period, where the mass-to-charge ratio is lower. During the next phase, which is equivalent to the higher rates of polymer deposition, there is a

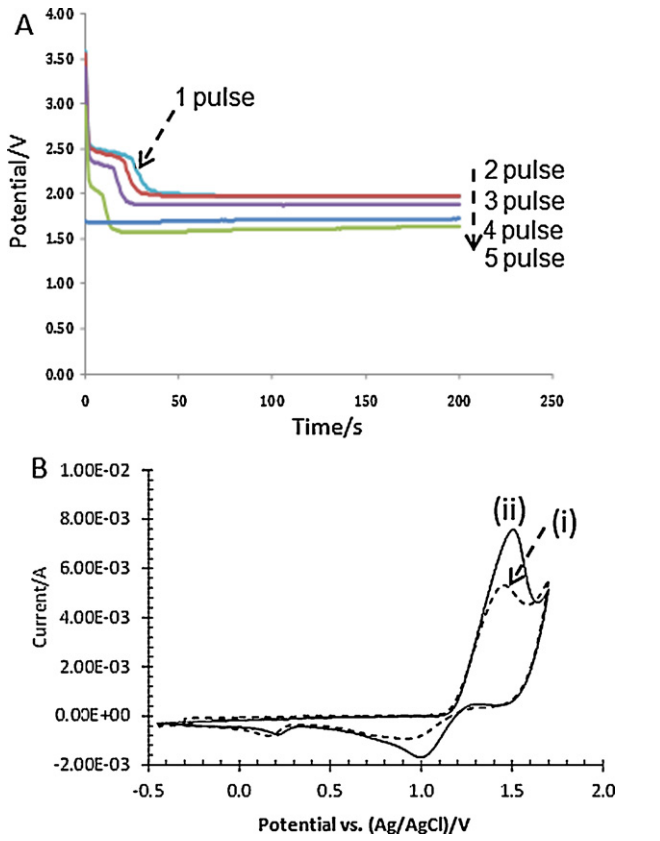

Fig. 9. Galvanostatic plot (A) recorded at 0.10 mA cm^{-2} with the application of pulse 1, pulse 2, pulse 3, pulse 4 and pulse 5, in the presence of 0.10 M NaVPA and 0.10 M Py. Each pulse was applied for 200 s with a rest of 60 s between each pulse utilising the gold coated Mylar as the working electrode. Redox properties (B) of 0.05 M NaVPA (i) and 0.05 M acetic acid (ii) at a scan rate of 25 mV s^{-1} using gold coated Mylar as the working electrode. The pH of the solutions was measured to be 7.3 and 2.7 for NaVPA and acetic acid respectively.

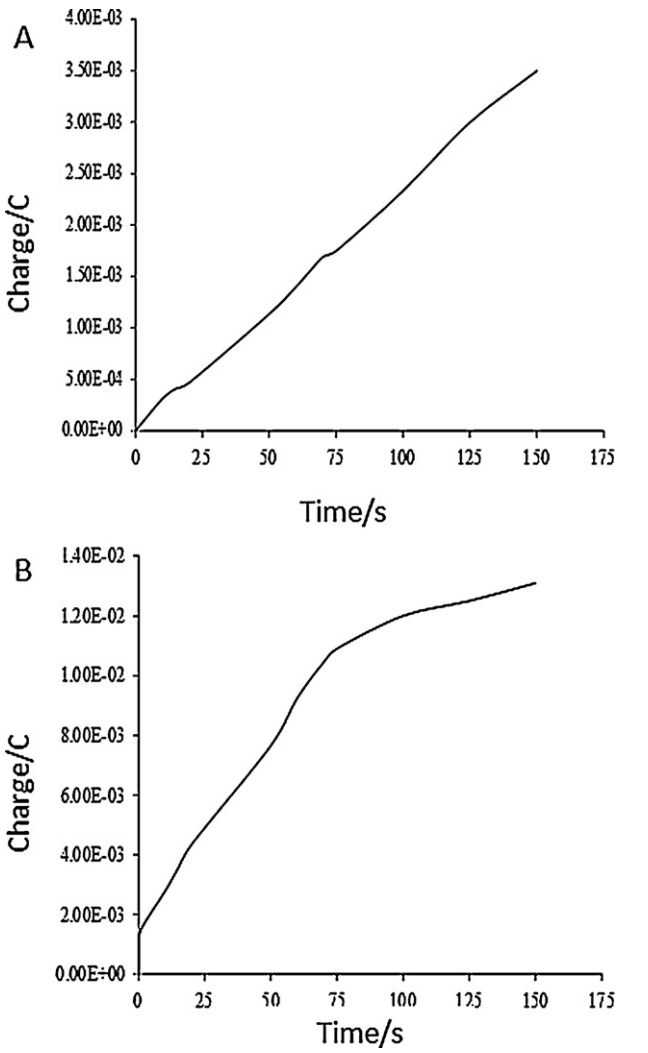

Fig. 10. Charge–time plots of the first 150 s of the attempted formation of VPA^{-} doped PPy by constant potential from a solution of 0.10 M NaVPA and 0.20 M Py. Constant potential of 0.90 V vs. Ag|AgCl was applied for polymerisation of Py on the bare gold coated Mylar electrode and on a PPypTS layer (B).

linear increase in charge with time, Fig. 9, in agreement with the data recorded at the macro-electrode, Fig. 5B.

3.6. PPy doped with VPA^{-}

The formation of VPA^{-} doped PPy was first attempted following a technique reported by Sabah et al. [43]. In that paper, the authors reported the preparation of a PPy film doped with VPA^{-} using a pulsed galvanostatic technique, where the polymer was deposited at platinum in 0.10 M NaVPA and 0.10 M Py with the application of five pulses, each 200 s, at 0.10 mA cm^{-2} with a rest of 60 s between each pulse. However, they did not show any data to prove that this polymer was formed. As shown in Fig. 9A, very high potentials were reached during each pulse, and upon visual observation no polymer film was evident. The potential increased from 1.70 V vs. Ag|AgCl at pulse 1 to an initial potential of 3.50 V vs. Ag|AgCl at pulse 5 which then settled at 1.90 V vs. Ag|AgCl. At these high potentials, the VPA^{-} is no longer stable and becomes oxidised, as shown in Fig. 9B. The cyclic voltammogram of acetic acid is also shown, indicating that the VPA oxidises at a similar potential. Also, at these electropositive potentials oxygen evolution occurs due to the oxidation of H_2O, Eq. (6). These oxidation reactions will prevent the electrodeposition of PPy at the electrode surface.

$$2H_2O \rightarrow O_2 + 4e^- + 4H^+ \quad (6)$$

In an attempt to control the potential of the electrode and maintain it below the oxidation potential of VPA^{-}, constant potential measurements were carried out to form the PPyVPA. Fig. 10A shows the charge–time plots recorded during the first 150 s of the application of a constant potential of 0.90 V vs. Ag|AgCl, in the presence of 0.10 M NaVPA and 0.20 M Py. Although there is an increase in the charge consumed, a polymer film was not observed. The electropolymerisation period was extended to 50 min, but again, no polymer was visible on the electrode surface. Slightly higher charges were measured when the electropolymerisation was attempted on a prelayer of PPypTS, Fig. 10B. FTIR–ATR analysis showed no spectral band associated with the presence of VPA, namely a band or shoulder at 1580 cm^{-1} attributed to carboxylic acid stretch (COONa) [44]. This suggests no PPyVPA was deposited on the surface of the electrode even after 50 min. A PPypTS polymer was analysed by FTIR–ATR after being immersed in a solution of 0.10 M NaVPA for 60 min followed by rinsing with MilliQ water for 30 s. Whilst the FTIR–ATR spectra was dominated by the bands associated with PPypTS a slight shoulder at approximately 1580 cm^{-1} was evident suggesting the presence of adsorbed VPA. This adsorbed VPA could hinder the electrochemical polymerisation of the PPyVPA polymer similar to that reported by Thompson et al. [35] for NT-3. Although no PPyVPA polymer was visible on the electrode surface, it is clear from Fig. 9 that some oxidation of the monomer takes place. This oxidation may induce formation of dimers and other soluble oligomers on application

of the constant potential, however further progression of the electropolymerisation process does not occur, possibly due to the adsorbed VPA layer. Polymerisation was attempted in a water/acetonitrile mix (ranging from 90/10, 80/20, 70/30, 60/40 and 50/50) with no success. Polymerisation was also attempted in pure acetonitrile and ethanol with the same result. Co-solvent of low concentration phosphate buffer saline (0.05 M) was tested, unfortunately polymer growth was problematic and in all instances no polymer formation was observed.

The pH of the electrolyte was varied in an attempt to electrosynthesise the PPyVPA directly onto the Pt electrode. The pH of the NaVPA-Py electrolyte was measured at 7.5. This was lowered to 6.2 and then further to 5.6 using HCl. The pH could not be lowered any further as the addition of the acid shifted the equilibrium to the undissociated HVPA acid which is insoluble in water, Eq. (7).

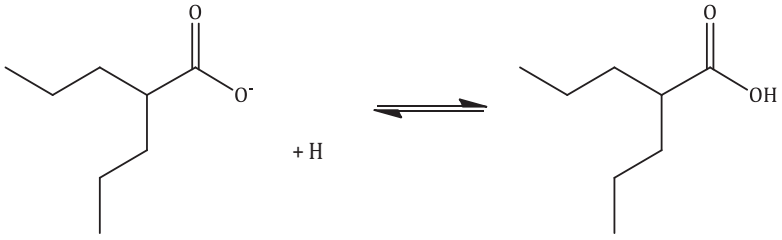

(7)

In order to shift the equilibrium further towards the soluble form of the VPA, the pH was increased with the addition of 5×10^{-4} M histamine (HA). HA has two centres that can be protonated, the aliphatic amino group, p$K_a \sim 9.4$, and the proton free nitrogen of the imidazole ring, p$K_a \sim 5.8$ [41]. The aliphatic amino group is readily protonated and in the presence of the HA, the VPA will exist as the anionic species, Eq. (8). The pH was then increased to 8.2 and then further to 9.3 with HA. Electropolymerisation was attempted at all five pH values (namely 5.6, 6.2, 7.5, 8.2 and 9.3) by sweeping the potential between −0.20 V vs. SCE and +1.20 V vs. SCE at a scan rate of 25 mV s^{-1}. However, electropolymerisation failed. This is not surprising as electropolymerisation of Py at pH values higher than 8.0 is difficult [17,28] but the fact that HVPA is insoluble at pH values lower than 5.6 means it is not possible to reduce the pH.

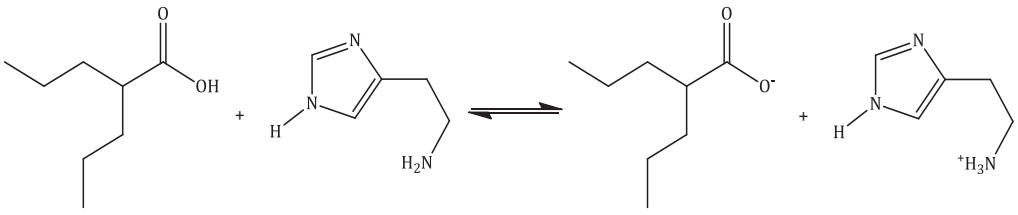

(8)

As evident in Fig. 2, the % of VPA^- anions in solution is 94% at pH 7.5, and the equilibrium favours the anionic form of VPA, however, at pH 5.0 the % of VPA^- anions is only 55%, while the insoluble HVPA is present at a nearly equal ratio. HVPA has a higher pK_a than HDF and its equilibrium is shifted towards its insoluble form at higher pH, as shown clearly in Fig. 2. It is likely that the local pH changes that affect the deposition of PPyDF have an even greater effect on the formation of PPyVPA. In the case of the PPyDF, some deposition of the polymer occurs prior to the formation of the insoluble drug crystals but, in the VPA^- case, it seems that during the initial oxidation of the monomer to generate soluble dimers and oligomers, the equilibrium shifts towards acidic conditions and causes insoluble HVPA to form at the electrode and this prevents the deposition of any PPyVPA.

4. Conclusions

This work demonstrates the significant influence of the pK_a of the acidic form of the dopant on the electropolymerisation of Py using diclofenac sodium salt and valproic acid sodium salt as model systems. Several attempts to deposit PPy doped with the anionic VPA^-, using constant potential, pulsed galvanostatic and cyclic voltammetry, failed to generate the polymer film. This was attributed to an increase in the concentration of protons in the vicinity of the electrode as the Py monomer is oxidised, which in turn, gives rise to a shift in the equilibrium between the anionic and acid forms towards the insoluble HVPA.

During the electrodeposition of PPyDF, the local acidity at the electrode causes insoluble drug crystals to form which hinders the rate of electropolymerisation, however, there is a sufficient concentration of the anionic DF^- species to dope the polymer. The difference in pK_a between HVPA and HDF, even though small, means that this local acidity has an even greater effect on the formation of PPy doped with VPA^- and prevents any polymer deposition from taking place. It appears that although the monomer is oxidised, there are no soluble anions available at the electrode interface to dope the polymer.

Acknowledgements

The authors would like to acknowledge funding from the Irish Research Council for Science, Engineering and Technology (IRCSET), the Endeavour Research Fellowship and the Australian Research Council. GGW and SEM wish to acknowledge the Australian Research Council for their Laureate Fellowship and QEII Fellowship respectively.

References

[1] J. Simonet, J. Rault-Berthelot, Progress in Solid State Chemistry 21 (1991) 1.
[2] T.F. Otero, E. De Larreta, Synthetic Metals 26 (1988) 79.
[3] T. Hernandez-Perez, M. Morales, N. Batina, M. Salmon, Journal of the Electrochemical Society 148 (2001) C369.
[4] M.D. Levi, C. Lopez, E. Vieil, M.A. Vorotyntsev, Electrochimica Acta 42 (1997) 757.
[5] E. Beelen, J. Riga, J.J. Verbist, Synthetic Metals 41 (1991) 449.
[6] J. Chengyou, Y. Fenglin, Y. Weishen, Journal of Applied Polymer Science 101 (2006) 2518.

[7] S. Jing, T.-S. Jadranka, C. Shu Yi, L. Kwong Chi, A.K. Paul, Journal of Applied Polymer Science 111 (2009) 876.
[8] H. Masuda, D.K. Asano, Synthetic Metals 135 (2003) 43.
[9] L. Sheng, Q. Yubing, G. Xingpeng, Journal of Applied Polymer Science 114 (2009) 2307.
[10] M. Vorotynsev, E. Vieil, J. Heinze, Journal of Electroanalytical Chemistry 450 (1998) 121.
[11] Y. Li, J. Yang, Journal of Applied Polymer Science 65 (1997) 2739.
[12] S. Sadki, P. Schottland, N. Brodie, G. Sabourand, Royal Society of Chemistry 29 (2000) 283.
[13] M. Satoh, K. Imanishi, K. Yoshino, Journal of Electroanalytical Chemistry 317 (1991) 139.
[14] M. Zhou, J. Heinze, Journal of Physical Chemistry B 103 (1999) 8443.
[15] S. Asavapiriyanont, G.K. Chandler, G.A. Gunawardena, D. Pletcher, Journal of Electroanalytical Chemistry 177 (1984) 229.
[16] T.F. Otero, J. Rodríguez, Electrochimica Acta 39 (1994) 245.
[17] S. Shimoda, E. Smela, Electrochimica Acta 44 (1998) 219.
[18] K. Kontturi, L. Murtomäki, P. Pentti, G. Sundholm, Synthetic Metals 92 (1998) 179.
[19] D.L. Gardner, Journal of Anatomy 184 (1994) 465.
[20] S. Dreve, I. Kacso, I. Bratu, E. Indrea, Journal of Physics: Conference Series (2009) 182.
[21] M. Hamidi, P. Rafiei, A. Azadi, S. Mohammadi-Samani, Journal of Pharmaceutical Sciences 100 (2011) 1702.
[22] M. Tuncay, S. Calis, H.S. Kas, M.T. Ercan, I. Peksoy, A.A. Hincal, Journal of Microencapsulation 17 (2000) 145.
[23] K. Manjunatha, M. Ramana, D. Satyanarayana, Indian Journal of Pharmaceutical Sciences 69 (2007) 384.
[24] M. Kammerer, M. Fabritius, C. Carvalho, R.J. Mülhaupt, T.J. Feuerstein, R. Trittler, Die Pharmazie—An International Journal of Pharmaceutical Sciences 66 (2011) 511.
[25] G. Zotti, S. Cattarin, N. Comisso, Journal of Electroanalytical Chemistry 235 (1987) 259.
[26] S.B. Saidman, J.B. Bessone, Journal of Electroanalytical Chemistry 521 (2002) 87.
[27] A.S. Liu, M.A.S. Oliveira, Journal of Brazilian Chemistry Society 18 (2007) 143.
[28] A.F. Diaz, J.I. Castillo, J.A. Logan, W.-Y. Lee, Journal of Electroanalytical Chemistry 129 (1981) 115.
[29] A.M. Fenelon, C.B. Breslin, Corrosion Science 45 (2003) 2837.
[30] J.M. Ko, H.W. Rhee, S.M. Park, C.Y. Kim, Journal of Electrochemistry Society 137 (1990) 905.
[31] C. Malitesta, F. Palmisano, L. Torsi, P.G. Zambonin, Analytical Chemistry 62 (1990) 2735.
[32] J.M. Elliott, L.M. Cabuché, P.N. Bartlett, Analytical Chemistry 73 (2001) 2855.
[33] M. Bazzaoui, L. Martins, E.A. Bazzaoui, J.I. Martins, Electrochimica Acta 47 (2002) 2953.
[34] N.C.T. Martins, T.M.E. Silva, M.F. Montemor, J.C.S. Fernandes, M.G.S. Ferreira, Electrochimica Acta 53 (2008) 4754.
[35] B.C. Thompson, S.E. Moulton, J. Ding, R. Richardson, A. Cameron, S. O'Leary, G.G. Wallace, G.M. Clark, Journal of Controlled Release 116 (2006) 285.
[36] E.M. Genies, G. Bidan, A.F. Diaz, Journal of Electroanalytical Chemistry 149 (1983) 101.
[37] J. Heinze, B.A. Frontana-Uribe, S. Ludwig, Chemical Review 110 (2010) 4724.
[38] C.S.C. Bose, S. Basak, K. Rajeshwar, The Journal of Physical Chemistry 96 (1992) 9899.
[39] S.B.I. Jureviciute, A.R. Hillman, A. Jackson, Physical Chemistry 2 (2000) 4193.
[40] T. Matencio, J.M. Pernaut, E. Vieil, Journal of Brazilian Chemistry Society 14 (2003) 90.
[41] P.L. Runnels, J.D. Joseph, M.J. Logman, R.M. Wightman, Analytical Chemistry 71 (1999) 2782.
[42] G. Sauerbrey, Zeitschrift für Physik 155 (1959) 206.
[43] S. Sabah, M. Aghamohammadi, N. Alizadeh, Sensors and Actuators B: Chemical 114 (2005) 489.
[44] S. Lankalapalli, R.M. Kolapalli, Drug Development and Industrial Pharmacy 38 (2012) 815.